




^{68}Ga -PSMA-11 PET has the potential to improve patient selection for extended pelvic lymph node dissection in intermediate to high-risk prostate cancer

Daniela A. Ferraro¹ · Urs J. Muehlematter^{1,2} · Helena I. Garcia Schüler³ · Niels J. Rupp⁴ · Martin Huellner¹ · Michael Messerli¹ · Jan Hendrik Rüschoff⁴ · Edwin E. G. W. ter Voert¹ · Thomas Hermanns⁵ · Irene A. Burger^{1,6} 

Received: 20 April 2019 / Accepted: 26 August 2019 / Published online: 14 September 2019
© Springer-Verlag GmbH Germany, part of Springer Nature 2019

Abstract

Introduction Radical prostatectomy with extended pelvic lymph node dissection (ePLND) is a curative treatment option for patients with clinically significant localised prostate cancer. The decision to perform an ePLND can be challenging because the overall incidence of lymph node metastasis is relatively low and ePLND is not free of complications. Using current clinical nomograms to identify patients with nodal involvement, approximately 75–85% of ePLNDs performed are negative. The aim of this study was to assess the added value of ^{68}Ga -PSMA-11 PET in predicting lymph node metastasis in men with intermediate- or high-risk prostate cancer.

Methods ^{68}Ga -PSMA-11 PET scans of 60 patients undergoing radical prostatectomy with ePLND were reviewed for qualitative (visual) assessment of suspicious nodes and assessment of quantitative parameters of the primary tumour in the prostate (SUV_{max} , total activity ($\text{PSMA}_{\text{total}}$) and PSMA positive volume (PSMA_{vol})). Ability of quantitative PET parameters to predict nodal metastasis was assessed with receiver operating characteristics (ROC) analysis. A multivariable logistic regression model combining PSA, Gleason score, visual nodal status on PET and primary tumour $\text{PSMA}_{\text{total}}$ was built. Net benefit at each risk threshold was compared with five nomograms: MSKCC nomogram, Yale formula, Roach formula, Winter nomogram and Partin tables (2016).

Results Overall, pathology of ePLND specimens revealed 31 pelvic metastatic lymph nodes in 12 patients. ^{68}Ga -PSMA-11 PET visual analysis correctly detected suspicious nodes in 7 patients, yielding a sensitivity of 58% and a specificity of 98%. The area under the ROC curve for primary tumour SUV_{max} was 0.70, for $\text{PSMA}_{\text{total}}$ 0.76 and for PSMA_{vol} 0.75. The optimal cut-off for nodal involvement was $\text{PSMA}_{\text{total}} > 49.1$. The PET model including PSA, Gleason score and quantitative PET parameters had a persistently higher net benefit compared with all clinical nomograms.

Conclusion Our model combining PSA, Gleason score and visual lymph node analysis on ^{68}Ga -PSMA-11 PET with $\text{PSMA}_{\text{total}}$ of the primary tumour showed a tendency to improve patient selection for ePLND over the currently used clinical nomograms.

This article is part of the Topical Collection on Oncology—Genitourinary

Daniela A Ferraro and Urs J. Muehlematter shared first authorship

Electronic supplementary material The online version of this article (<https://doi.org/10.1007/s00259-019-04511-4>) contains supplementary material, which is available to authorized users.

✉ Irene A. Burger
Irene.Burger@usz.ch

¹ Department of Nuclear Medicine, University Hospital Zurich, University of Zurich, Rämistrasse 100, 8091 Zürich, Switzerland

² Institute of Diagnostic and Interventional Radiology, University Hospital Zurich, University of Zurich, Zurich, Switzerland

³ Department of Radiation Oncology, University Hospital Zurich, University of Zurich, Zurich, Switzerland

⁴ Department of Pathology and Molecular Pathology, University Hospital Zurich, University of Zurich, Zurich, Switzerland

⁵ Department of Urology, University Hospital Zurich, University of Zurich, Zurich, Switzerland

⁶ Department of Nuclear Medicine, Kantonsspital Baden, Baden, Switzerland

Although this result has to be validated, ^{68}Ga -PSMA-11 PET showed the potential to reduce unnecessary surgical procedures in patients with intermediate- or high-risk prostate cancer.

Keywords SUV_{max} · PET quantification · Lymph node metastases · PET/MR · PET/CT · Staging · Prediction model · Nomogram · Net benefit

Abbreviations

RPE	Radical prostatectomy
ePLND	Extended pelvic lymph node dissection
RT	Radiotherapy
LNM	Lymph node metastasis
CT	Computed tomography
PET	Positron emission tomography
^{68}Ga -PSMA-11 PET	Positron emission tomography with prostate-specific membrane antigen
^{68}Ga -PSMA-11	^{68}Ga -PSMA-11 PET/magnetic resonance imaging
PET/MRI	resonance imaging
PSA	Prostate-specific antigen
GS	Gleason score
MSKCC	MSKCC nomogram
YF	Yale formula
RF	Roach formula
WN	Winter nomogram
PT (2016)	Partin tables
SD	Standard deviation
SUV_{max}	Standard uptake value
PSMA_{vol}	PSMA positive volume
$\text{PSMA}_{\text{total}}$	PSMA accumulation
ROC	Receiver operating characteristics
AUC	Area under the ROC curve
NB	Net benefit
EIP	Irradiation of the pelvic nodes
CI	95% Confidence interval

Background

Radical prostatectomy (RPE) and extended pelvic lymph node dissection (ePLND) or local radiotherapy (RT) with or without the inclusion of the lymphatic drainage are the current treatments of choice for patients with clinically significant and localised prostate cancer. According to the guidelines, ePLND is performed in most patients with intermediate- and high-risk disease [1], although an oncological benefit of LN removal has never been confirmed. ePLND is associated with potential complications, such as lymphoceles, lymph edema and thromboembolic events. Furthermore, it is also prolonging the operation time and therefore increasing costs [2, 3].

Given the relatively low incidence of lymph node metastasis (LNM) of around 4% in patients diagnosed with prostate

cancer [4] and the implied morbidity risk of ePLND, numerous efforts have been made to predict LN metastasis for improved patient selection. Imaging did not reach satisfactory detection of micro-metastasis: computed tomography (CT) showed a sensitivity of only 13% in a study with 1541 patients [5] and MRI showed sensitivity of 39% in a meta-analysis [6]. The combination of radiographic and nuclear medicine techniques in positron emission tomography (PET) with ^{18}F - or ^{11}C -Choline reached a sensitivity of only 49–59% [7, 8]. Furthermore, sentinel node biopsy did not gain widespread acceptance, mostly due to logistic difficulties and aberrant paths of drainage [9]. Therefore, prostate cancer centres perform ePLND based on clinical nomograms, incorporating several clinical risk factors to predict LNM, even in the absence of positive findings on staging imaging [10, 11]. However, the decision to perform an ePLND is still difficult and depends on the cut-off chosen for suspected nodal involvement. To prevent understaging of patients, guidelines usually recommend lymphadenectomy to all high-risk patients and rather low cut-offs for intermediate-risk patients such as 5% in the European Association of Urology Guideline [1] and 2% in the National Comprehensive Cancer Network Guideline [12], at the cost of unnecessary lymphadenectomies in around at least 75–85% of the patients [13–15].

Lately, the performance of PET with prostate-specific membrane antigen (^{68}Ga -PSMA-11 PET) in detecting metastatic lymph nodes was assessed in multiple studies and recently reviewed in a meta-analysis resulting in a sensitivity of 51–89% [16, 17]. In a study comparing ^{68}Ga -PSMA-11 PET/magnetic resonance imaging (^{68}Ga -PSMA-11 PET/MRI) with currently available clinical nomograms to predict LNM, Thalgot et al. found that the visual detection of nodal metastasis was comparable with the nomograms [17]. However, the spatial resolution of PET limits its detection rate for micro-metastasis, being probably the reason behind the still suboptimal sensitivity.

Furthermore, assessment of the primary tumour by molecular imaging may be a potential tool to predict nodal metastasis in cancer patients. Based on the fact that PSMA has been shown to correlate with risk groups and Gleason score (GS) [18–21], it is reasonable to assume that PSMA uptake in the primary tumour could predict distant disease. In fact, some authors already presented at EANM 2018 that a maximum standard uptake value (SUV_{max}) cut-off of 19.9 can predict distant lesions seen on ^{68}Ga -PSMA-11 PET [22]. Whether quantitative parameters of the primary tumour on ^{68}Ga -

Table 1 Clinical information used in clinical prediction models

Models	PSA	GS	Clinical stadium	Number of positive and negative biopsy cores	Age	Reference
MSKCC [24]	X	X	X	X	X	Histo
RF [26]	X	X				Histo
YF [25]	X	X	X			Histo
WN [27]	X	X	X			Histo
PT [28]	X	X	X			Histo
D'Amico score	X	X	X			Outcome

PSMA-11 PET could predict metastatic disease has not yet been investigated.

The aim of this study was to investigate whether a combination of qualitative and quantitative parameters on ^{68}Ga -PSMA-11 PET could predict LNM in patients with intermediate or high-risk prostate cancer and assess the added value of ^{68}Ga -PSMA-11 PET in comparison with current clinical nomograms for risk assessment of nodal disease.

Patients and methods

Study population

This retrospective study included all patients that underwent ^{68}Ga -PSMA-11 PET for staging of prostate cancer prior to radical prostatectomy with ePLND between April 2016 and August 2018 in our institution. ePLND is a standard procedure for all intermediate- and high-risk prostate cancer patients that undergo RPE in our hospital. The local ethics committee approved the study protocol and all patients gave a general written informed consent for retrospective use of their data (BASEC Nr. 2018-01284).

Study design

We retrospectively reviewed the ^{68}Ga -PSMA-11 PET scans and obtained information from the pathological report of the RPE and ePLND of all patients. Scans were reviewed in order to assess the presence of PSMA-expressing lymph nodes suspicious for metastasis and obtain quantitative PET parameters of the primary tumour. Data collected from the pathological reports included number and location of metastatic lymph nodes in addition to largest diameter of the metastasis. Relevant clinical information was collected from patient charts such as age, clinical TNM stage, D'Amico risk score, prostate-specific antigen (PSA) value at scan time, biopsy GS and number of positive and negative cores, and was used to fill the nomograms to assess probability of LNM for each patient.

Risk of LNM was calculated based on nomograms and their performance was assessed using histopathology of the

lymphadenectomy as standard of truth. Five nomograms were selected based on their performance on previous studies [23]: MSKCC nomogram (MSKCC) [24], Yale formula (YF) [25], Roach formula (RF) [26], Winter nomogram (WN) [27] and Partin tables (2016) (PT) [28]. D'Amico score, despite developed to assess risk of recurrence [29], has commonly been also used to assess risk of nodal involvement, and was therefore included in this study. Information regarding D'Amico score and the nomograms is shown in Table 1.

MSKCC MSKCC nomogram, *YF* Yale formula, *RF* Roach formula, *WN* Winter nomogram, *PT* Partin tables (2016), *PSA* prostatic specific antigen, *GS* Gleason score

Imaging techniques

Patients underwent ^{68}Ga -PSMA-11 PET/MR ($n = 46$) if no MR contraindications were present and PET/MR slots were available, or ^{68}Ga -PSMA-11 PET/CT ($n = 14$) after a single injection of ^{68}Ga -PSMA-11 (mean dose \pm standard deviation (SD), 133 ± 18 MBq). To reduce tracer activity in the bladder, ureters and kidneys, furosemide was injected intravenously 30 min prior to the tracer injection (0.13 mg/kg) and patients were asked to void prior to the scan. The institutional protocol is in agreement with the EANM and SNMMI procedure guidelines [30].

PET/MR protocol

A clinical routine partial-body PET/MR was performed 60 min after injection on a hybrid scanner (SIGMA PET/MR, GE Healthcare, Waukesha, WI, USA) used in previous studies at our department with the same protocol for prostate imaging as recently described [31]; in brief, six bed positions with 2–3 min acquisition time per bed position for the whole-body protocol and additional specific sequences covering the pelvis, including a high-resolution T1-weighted fast spoiled gradient-echo sequence (LAVA Flex) and T2-weighted fast recovery fast spin-echo sequence (FRFSE) in at least two planes.

PET/CT protocol

For patients who underwent a PET/CT, PET was performed with six bed positions with 2.5 min acquisition time per bed position and an attenuation CT scan was acquired on a Discovery VCT 690 PET/CT (GE Healthcare, Waukesha, WI, USA) or on a Discovery MI PET/CT (GE Healthcare, Waukesha, WI, USA), 60 min after injection with whole-body scan parameters as follows: tube voltage 140 kV, tube current with automated dose modulation with a maximum of 80 mA/slice, collimation 512×0.976 , pitch 0.984:1, rotation time 0.5 s, coverage speed 78 mm/s, field of view 50 cm and images with a transverse pixel size of 0.976 and a slice thickness of 1.25 mm reconstructed in the axial plane.

Imaging analysis

The acquired PET/CT and PET/MR images were analysed in a dedicated review workstation (Advantage Workstation, Version 4.6 or 4.7, GE Healthcare), which enables the review of the PET and the CT or MR images side by side and in fused mode. All scans were analysed in consensus by a dual board-certified radiologist and nuclear medicine physician with 10 years and a nuclear medicine physician with 4 years of experience, incorporating both the MRI or CT and PET information. The readers had access to clinical information for the

readouts. Qualitative assessment for LNM was done in consensus by the two readers. Care was taken to avoid false-positive findings by considering physiological biodistribution and the known PSMA positive pitfalls such as neural ganglia, Paget's disease, sarcoidosis and others [32, 33].

Quantitative parameters were assessed by delineating the PSMA-expressing tumours with an automatic algorithm based on a background-based threshold set to $SUV_{max} \geq 4$. The volume of interest was placed by two observers in consensus to fully include the primary tumour and exclude neighbouring tissues with high PSMA accumulation (e.g. urine). If needed, manual subtraction was performed for non-tumour parts that were automatically included into the tumour volume, such as urinary bladder. Tumours with low PSMA expression (below SUV_{max} 4), but still clearly distinguishable from background prostate tissue by visual analysis, had the SUV threshold lowered so that the selected tumour volume correctly covered the visual apparent lesion. Parameters SUV_{max} , the PSMA positive volume ($PSMA_{vol}$) and the total PSMA accumulation ($PSMA_{vol} \times SUV_{mean} = PSMA_{total}$) of the primary tumour were recorded as well as SUV_{max} of suspicious nodes.

Radical prostatectomy and lymphadenectomy

All surgical procedures were performed in form of a robot-assisted transperitoneal laparoscopic radical prostatectomy with bilateral ePLND by experienced urologists at our institution as described earlier [34]. All operations were performed using the four-arm Da Vinci SI system (Intuitive Surgical, Inc., USA). ePLND included the external iliac, obturator and internal iliac (hypogastric) lymph nodes with an upper resection boundary defined by the crossing of the ureter over the common iliac artery. It was performed in all included patients irrespective of the result of PSMA PET imaging. If PSMA PET revealed suspicious lymph nodes in the common iliac region, a super-extended pelvic lymph node dissection was performed on the respective side.

Statistical analysis

Descriptive statistics were used to display patient data as median, mean, standard deviation range and percentages. The predicted risk for LNM was assessed for each individual patient using clinical nomograms. Sensitivity, specificity, positive predictive value and negative predictive value for LNM were calculated using lymph node status from PET (LN_{status} , 1 = positive or 0 = negative by visual analysis). Univariable and multivariable logistic regression models were created for clinical and PET parameters to correlate with LNM. Two multivariable models were considered: one with only clinical parameters and one with clinical and PET parameters. Variables included in the two latter models were selected by using backward stepwise selection based on the Akaike information

Table 2 Patient's characteristics

Characteristics	Value
Age (years)	
Mean \pm SD	64 \pm 6
Median (range)	65 (51–79)
PSA at time of PET scan (ng/ml)	
Mean \pm SD	13 \pm 13.6
Median	9 (1–78)
Gleason score ISUP group [39] <i>n</i> (%)	
2	6 (10%)
3	10 (17%)
4	27 (45%)
5	17 (28%)
Initial clinical T Staging <i>n</i> (%)	
T1a	1 (2%)
T1b	0
T1c	37 (62%)
T2a	9 (15%)
T2b	2 (3%)
T2c	11 (18%)
D'Amico score <i>n</i> (%)	
High risk	52 (87%)
Intermediate risk	8 (13%)

Table 3 Univariable and multivariable logistic regression model for lymph node metastasis prediction

Variable (unit)	OR	95% CI	<i>p</i> value
Univariable logistic regression model			
Age (year)	0.96	0.87–1.07	0.45
cT (1–6)*	0.74	0.40–1.35	0.32
Gleason (2–5)†	1.76	0.79–3.93	0.17
PSA (ng/ml)	1.07	1.01–1.12	0.02*
SUV _{max} (–)	1.06	1.00–1.13	0.04*
PSMA _{vol} (cm ³)	1.16	1.04–1.29	0.008**
PSMA _{total} (–)	1.02	1.01–1.04	0.009**
LN _{status} (positive LN)	65.80	6.67–649.23	<0.001***
Multivariable logistic regression model			
Clinical parameters (AIC = 53.48)			
Intercept	0.003	0–0.13	0.009**
- Gleason score (2–5)†	2.72	1.02–7.21	0.04*
- PSA (ng/ml)	1.10	1.02–1.17	0.008**
Clinical + PET parameters (AIC = 36.06)			
Intercept	0.001	0–0.08	0.009**
- Gleason score (2–5)†	4.61	0.84–25.24	0.08
- PSA (ng/ml)	1.10	0.99–1.02	0.06
- LN _{status} (positive LN)	170.4	7.20–4032.54	0.001**
- PSMA _{total} (–)	1.02	0.99–1.04	0.15

Odds ratio (OR) is given by 1-unit change. Significance codes: 0 = ***, 0.001 = **, 0.01 = *. Akaike information criterion (AIC), * cT (1–6; T1a = 1; T1b = 2; T1c = 3; T2a = 4; T2b = 5; T2c = 6)

† According to ISUP groups

criterion from clinical (age, clinical T stage (cT), GS and PSA) and imaging parameters (SUV_{max}, PSMA_{total}, PSMA_{vol}). Diagnostic performance of the nomograms and of the multivariable models was quantified by area under the receiver operating characteristics (ROC) curve (AUC). The two multivariable models were evaluated using a 10 times repeated 5-fold cross-validation. AUC between the two nested multivariable models was compared with the likelihood ratio test [35]. Clinical utility of each prediction model and the results of the nomograms was assessed by a decision curve analysis in which net benefit (NB) was plotted against risk threshold for each prediction model along with the treat-none and treat-all strategy [36, 37]. NB at each risk threshold probability was defined as the difference between the proportion of true-positive results and weighted proportion of false-positive results with the weight equal to threshold probability/(1-threshold probability). The prediction model with the highest net benefit at a given risk threshold has the highest clinical value [38]. All tests were two sided and *P* values ≤ 0.05 were considered statistically significant. All statistical and graphical analysis was performed in R (version 3.5.1; R Foundation for Statistical computing, Vienna, Austria).

Results

A total of 60 patients were enrolled. Mean age was 64 years (SD ± 6) and PSA levels ranged from 1 to 78 ng/ml with median of 9 ng/ml. All patients had clinical T1 or T2 stadium, with the majority being staged as cT1c (37/60, 62%). Biopsy GS ranged from 3 + 4 = 7 to 5 + 4 = 9, with 4 + 4 = 8 being the most frequent (*n* = 26, 43%). Overall, 52 patients (87%) had high-risk and 8 patients had intermediate-risk (13%) prostate cancer according to D'Amico classification. Nine of the patients had sextant or dodecant biopsies only and 45 patients had template saturation biopsies with or without additional multiparametric MRI-guided lesion biopsies (median of 40 cores). In 5 patients, prostate cancer was diagnosed by MRI targeted-biopsy only, with no systematic biopsy performed, and in one patient by transurethral prostate resection (TURP). For those 6 patients, MSKCC nomogram was calculated without the number of positive biopsy cores. Details regarding patient characteristics are shown in Table 2.

⁶⁸Ga-PSMA-11 PET visual analysis detected positive lymph nodes in 8 patients, with a mean SUV_{max} of 9.0 (SD ± 4.6), being in one patient a false-positive. Most nodes were localised in the pelvis; however, in 2 patients, distant nodes were found in the common iliac chain. The primary tumour was PSMA-negative in 3 patients (5%), none of these patients had suspicious nodes on ⁶⁸Ga-PSMA-11 PET nor histologically proven LNM. Mean SUV_{max} of the primary tumour for the other 57 patients was 15 (SD ± 10), mean PSMA_{total} and PSMA_{vol} were 53 (SD ± 66) and 8 cm³ (SD ± 6.6), respectively

Mean interval between ⁶⁸Ga-PSMA-11 PET and RPE was of 1.8 months (SD ± 2.26). The median number of surgically removed lymph nodes per patient was 21 (range 12–68). Overall, 31 metastatic pelvic lymph nodes were found in 12 (20%) patients, with a median number of 2 positive nodes per patient (range from 1 to 7). Most nodes were localised in the external iliac chain and in 2 patients common iliac nodes were found, already seen on ⁶⁸Ga-PSMA-11 PET scan. ⁶⁸Ga-PSMA-11 PET was falsely negative in 5 patients, all of them with metastasis smaller than 2.5 mm. In one patient, ⁶⁸Ga-PSMA-11 PET was false-positive for an external iliac node (axial diameter 5 mm, SUV_{max} 4.8). All 12 patients with LNM were high-risk patients according to the D'Amico classification, 9 of them were clinically staged as T1c and 3 patients as T2. Median PSA level for those patients was 17 ng/ml (range 5–54 ng/ml) and biopsy GS varied from 3 + 4 = 7 to 5 + 4 = 9 with most of them having a GS 4 + 5 = 9 (5/12 patients).

Prediction of nodal involvement based on clinical parameters

Probability of LNM among all patients varied from 1 to 82% among all the five clinical nomograms. The 12 patients with

Table 4 AUC of clinical nomograms and multivariable logistic regression in the prediction of lymph node metastasis

Model	AUC (95% CI)
MSKCC	0.71 (0.55–0.87)
RF	0.83 (0.69–0.96)
YF	0.75 (0.57–0.93)
WN	0.62 (0.43–0.80)
PT	0.63 (0.41–0.84)
Multivariable logistic regression (clinical parameters)*	0.78 (0.74–0.82)
Multivariable logistic regression (clinical + PET parameters)**	0.90 (0.87–0.93)
Quantitative PET parameters	AUC (95% CI)
SUV _{max}	0.70 (0.54–0.85)
PSMA _{vol}	0.75 (0.58–0.92)
PSMA _{total}	0.76 (0.6–0.92)

*PSA, Gleason Score

**PSA, Gleason Score, LNstatus and PSMAtotal

LNM had a mean predicted risk value of 26% (SD ± 18%) and a median of 24% (range 2–82%), while for the group of 48 patients without LNM mean predicted risk value was 17% (SD ± 13%) and median 13% (range 1–63%). Overall RF yielded the best AUC among the nomograms of 0.83 (95% confidence interval (CI) = 0.69–0.96), followed by YF (AUC 0.75, CI = 0.57–0.93) and MSKCC (AUC 0.71, CI = 0.55–0.87). Applying the current approach recommended by

guidelines [1] of performing lymphadenectomy for all high-risk patients and intermediate-risk patients with more than 5% of probability of LNM according to RF, all patients in our cohort were candidates for ePLND.

In the univariate analysis of all clinical variables, only PSA was significantly associated with LNM (Table 3). The multivariable logistic regression model including PSA level and GS yielded an AUC of 0.78 (CI = 0.74–0.82). AUC values and

Fig. 1 ROC curves for the nomograms and prediction models based on clinical parameters (PSA and GS) and on clinical + PET parameters (PSA, GS, LN_{status} and PSMA_{total}). The model based on both clinical and PET information yielded the highest AUC (0.90, CI = 0.87–0.93), followed by RF (AUC 0.83, CI = 0.69–0.96) and the model based only on clinical parameters built from our cohort (AUC 0.78, CI = 0.74–0.82)

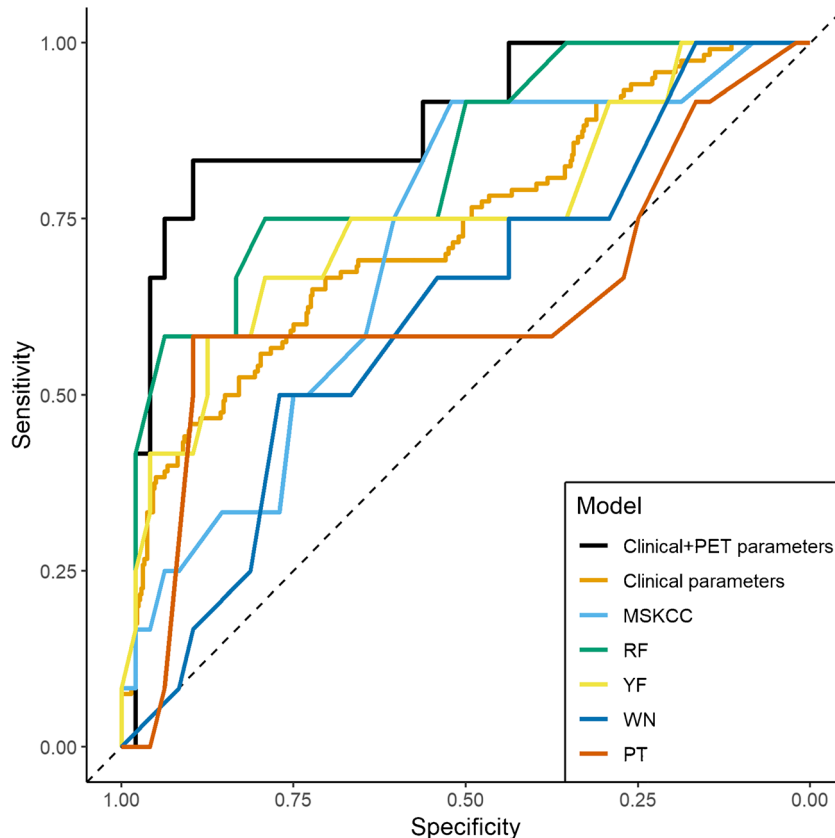
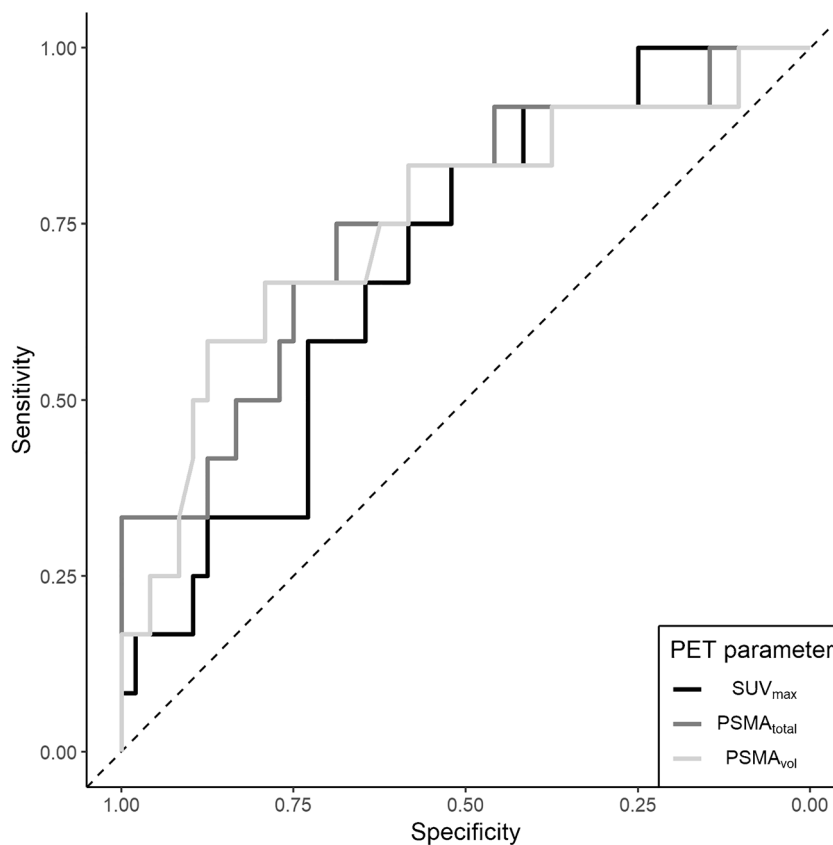


Fig. 2 ROC curves for the quantitative PET parameters. Among the quantitative PET parameters, PSMA_{total} yielded the highest AUC (0.76, CI = 0.6–0.92), followed by PSMA_{vol} (0.75, CI = 0.58–0.92) and SUV_{max} (AUC 0.70, CI = 0.54–0.85)



ROC curves for the nomograms and prediction models built from our cohort are shown in Table 4 and Fig. 1, respectively.

Prediction of nodal involvement including PET information

The patient-based sensitivity, specificity, positive predictive value and negative predictive value of PET visual analysis of lymph nodes were 58%, 98%, 88% and 90%, respectively. All three quantitative PET parameters from the primary tumour were significant predictors of LNM in the univariable analyses (Table 3) and correlated with nodal disease on histopathology with an AUC of 0.76 (CI = 0.6–0.92) for PSMA_{total}, 0.75 (CI = 0.58–0.92) for PSMA_{vol} and 0.70 (CI = 0.54–0.85) for SUV_{max}, not reaching statistically significant difference between them. The optimal threshold for PSMA_{total} calculated with the Youden index was 49.1 and for SUV_{max} 11.4. Figure 2 depicts the ROC analysis of the quantitative PET parameters.

The prediction model including PSA level, GS, visual analysis of LN_{status} and PSMA_{total} was most predictive for LNM (AUC 0.90, CI = 0.87–0.93). This model showed a better diagnostic performance compared with the model including only clinical parameters ($p = 0.003$). Figures 3 and 4 show examples of patients from our cohort that would be considered suspicious for having LNM based on LN_{status} and a high

primary tumour PSMA_{total}, respectively. Figure S1 in the supplementary material represents the nomogram of the final model including clinical and PET parameters.

Decision curve analysis

Our model including the two PET parameters (LN_{status} and PSMA_{total}), PSA level and GS had persistently higher net benefit (NB) compared with the clinical prediction model and to all nomograms for risk thresholds greater or equal to 7%. At a risk threshold of 15%, the difference of NB between the PET parameter model and the best performing clinical nomogram (i.e. PT) is 0.044 (0.146–0.102). Therefore, use of the PET parameter model would lead to 25% ($0.044 \times 100 / (0.15 / 0.85)$) fewer ePLND in patients without LNM with no increase in the number of patients with LNM left untreated, compared with the use of PT. Net benefits are depicted in Fig. 5.

Discussion

The results of our study indicate that risk prediction of LNM including information of qualitative and quantitative PET parameters for intermediate- and high-risk cancer patients has the potential to improve patient selection for ePLND. In our

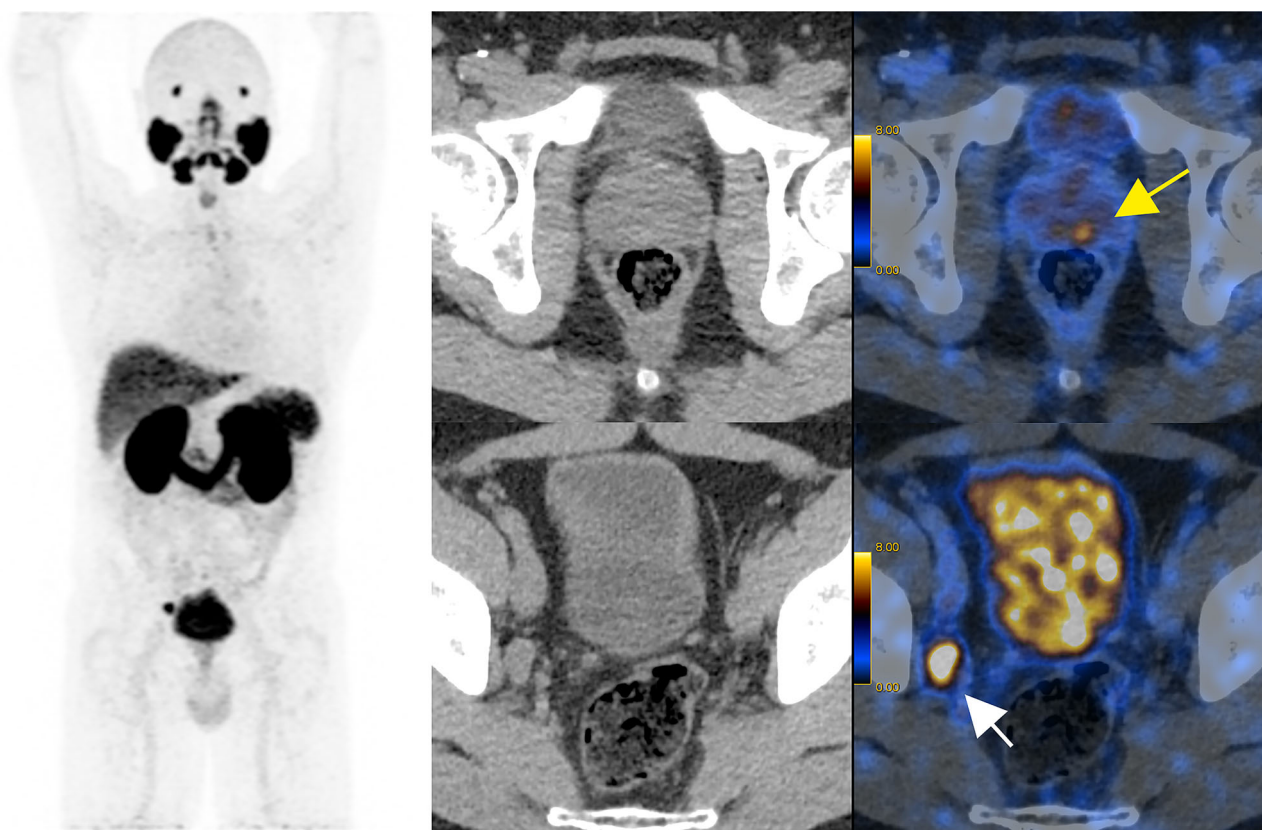


Fig. 3 Maximum intensity projection (MIP), CT and ^{68}Ga -PSMA-11 PET/CT fusion of a patient with a low PSMA-expressing primary tumour (GS 4 + 3 = 7, yellow arrow) with a SUV_{max} of 6 and a

PSMA_{total} of 3, but a highly PSMA-expressing 11-mm (short axis) internal iliac node (white arrow) with a SUV_{max} of 13. The node was confirmed as having a 2.4-cm metastasis on histopathology

cohort, a prediction model combining visual $\text{LN}_{\text{status}}$ on ^{68}Ga -PSMA-11 PET, PSMA_{total} of the primary tumour, PSA and GS yielded the highest AUC for LNM prediction with the highest net benefit between risk thresholds of 7–15%, showing potential to reduce futile ePLND.

Use of primary tumour PSMA uptake to predict nodal disease seen on PET has been previously shown [22]. Uslu-Besli et al. proposed a primary tumour SUV_{max} cut-off of 19.9 to predict positivity, by visual analysis, of lymph nodes on ^{68}Ga -PSMA-11. Our lower cut-off for SUV_{max} 11.4 most likely reflects that small lymph node metastasis detected by histopathology after lymphadenectomy occurs earlier in the process than positive nodes are seen on imaging. In our small cohort, PSMA_{total} of the primary tumour had a slightly higher AUC compared with SUV_{max} . The use of volume-based quantitative PET parameters of the primary tumour to predict LNM has not been investigated for prostate cancer yet and needs further confirmation. Interestingly, in some patients, PSMA expression is higher in the metastasis compared with the primary tumour (Fig. 3). This could be explained by the fact that primary prostate cancer can be a heterogeneous multifocal tumour [40]. In some cases, a small clone within the primary tumour with higher aggressiveness may be the origin of metastatic lesions [41, 42].

The currently used prediction models for LNM are based only on clinical factors (PSA, age, biopsy GS, T stage and number of positive and negative biopsy cores) and achieved superior results compared with all conventional imaging modalities so far. In a recent investigation comparing clinical nomograms and ^{68}Ga -PSMA-11 PET/CT in a cohort with pathology proven LNM in 34.3%, MSKCC nomogram performed better than ^{68}Ga -PSMA-11 PET/CT, predicting a prevalence of 39% of LNM while ^{68}Ga -PSMA-11 PET/CT detected lymph nodes in 20.6% of the patients [17]. Nevertheless, ^{68}Ga -PSMA-11 still offers the advantage of the localisation of a suspicious lesion, which can alter the surgical or radiation plan if the suspected lesion is not within the standard area of lymphatic drainage.

In concordance to the study from Briganti et al. [13] that reported a rate of 79% of futile pelvic nodal dissections using the 5% risk cut-off according to the nomogram as recommended by the guidelines [1], we had 80% futile ePLND in our cohort. This substantial number of patients undergoing more extensive surgery than needed leads to increased morbidity, longer operative room times and higher costs. On average, an ePLND adds 45–90 min operative time to a standard RPE without pelvic lymph node dissection and omitting futile ePLND can be expected to bring even further benefit due to

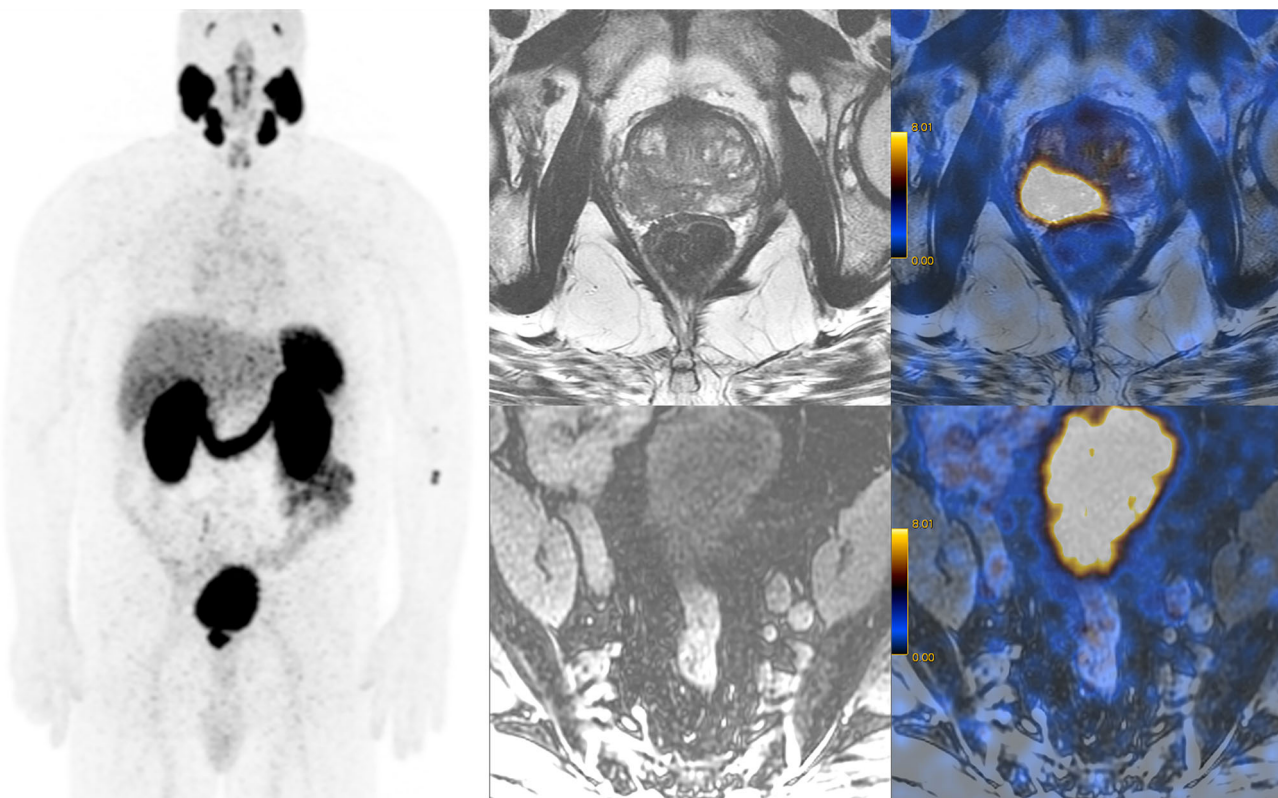


Fig. 4 MIP, axial MRI and ^{68}Ga -PSMA-11 PET/MRI fusion of a patient with a large and highly PSMA-expressing primary tumour in the right peripheral zone (upper row, T2 FRSE and fusion) with a SUV_{max} of 24 and a $\text{PSMA}_{\text{total}}$ of 109.5 and morphologically normal lymph nodes with

no PSMA expression (bottom row, water-only LAVA Flex and fusion). On histopathology, 3 positive external iliac nodes were found on the left side, with metastasis size up to 1.5 mm

prevention of additional costs related to histopathological analysis and side effects such as lymphocele, lymph edema and thromboembolic events.

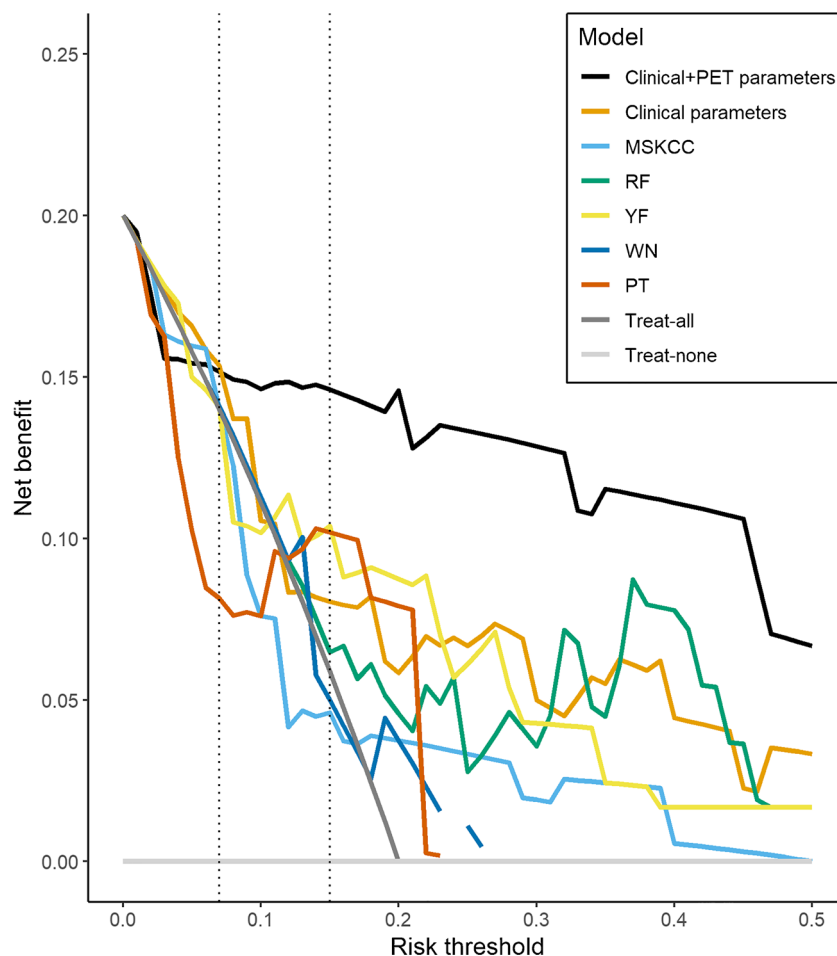
Also for patients undergoing definitive RT instead of surgery, a pre-therapeutic evaluation of the nodal risk and especially a potential localisation of macroscopic lesions would be beneficial. In clinical practice, elective irradiation of pelvic nodes (EIP) can be considered in high-risk patients undergoing primary RT, when nodal risk is estimated higher than 15%. This risk is usually assessed using the Roach formula [26], although criticised for overestimating the risk of LN involvement. Furthermore, EIP is still a controversial topic with some studies failing to show a benefit of EIP in cN0 patients [43] and others showing an improved progression free survival in patients who received EIP [44–46]. Although modern RT techniques as intensity-modulated RT and image-guidance reduce the toxicity of pelvic irradiation [47, 48], inclusion of pelvic nodes into the radiation field can lead to side effects, especially gastrointestinal ones [49]. Thus, patient selection is important to avoid overtreatment but remains a challenge.

On the other hand, when using a new prediction tool to select patients for treatment, the risk of undertreatment due to false-negatives has to be taken into consideration. For patients undergoing primary staging of prostate cancer, false-

negative results regarding LNM with omission of ePLND or radiation of pelvic nodes would lead to incomplete treatment and subsequent PSA persistence after radical prostatectomy or definitive RT. As recently reported by Thalgott et al. [17], visual analysis of nodes on PSMA PET is not superior enough to replace clinical nomograms in predicting LNM. However, our data show that assessment of quantitative PET parameters of the primary tumour might improve the sensitivity to detect LNM, reducing the number of false-negative PSMA PET scans, even though the best risk threshold based on quantitative PET parameters would still have to be established in a validation cohort for the assessment of false-negatives rates. Furthermore, the benefits and risks of ePLND were out of the scope of this study, remaining controversial in the light of actual literature [3, 50].

The main limitations of our study are the small sample size and its retrospective nature, which entails a selection bias. Therefore, the development of complex multivariable models is limited. Because of a limited number of cases, the data set was used for both fitting and evaluating prediction models, which may have caused bias in ROC analysis and decision curve analysis, leading to over-confidence in model performance. However, the model including PET parameters performed better even

Fig. 5 Decision curve analysis. For very low-risk thresholds, the clinical prediction models, as well as the model including ^{68}Ga -PSMA-11 PET parameters and the treat-all strategy, have close performances. However, for patients that the surgeon opts to perform an extended pelvic lymph node dissection if the risk of nodal metastasis is $\geq 7\%$, the model including ^{68}Ga -PSMA-11 PET information shows a higher net benefit compared with all clinical nomograms and the treat-all strategy



when compared with a clinical model also built with data from our cohort, which suggests ^{68}Ga -PSMA-11 PET information improves prediction of LNM over clinical information alone. Moreover, in our analyses, cT and GS were treated as continuous variables (to reduce the degrees of freedom and therefore reducing the risk of an overly optimistic model fit), inevitably leading to the assumption that the numerical distance between each set of subsequent categories is equal, which might not be true. Before preoperative ^{68}Ga -PSMA-11 PET staging can be recommended to be used in clinical practice to select patients for ePLND, our promising results need to be validated in a larger cohort of patients. However, there is still only scarce data for PSMA PET with histopathological confirmation and this is the first study that uses quantitative PET parameters for the evaluation of risk of LNM.

Conclusion

In our cohort, we could confirm that ^{68}Ga -PSMA-11 PET has a sensitivity for pelvic nodal metastasis of

58%. Considering $\text{PSMA}_{\text{total}}$ of the primary tumour as a risk factor for nodal involvement, a simple model including PSA level, GS, nodal status on PET and $\text{PSMA}_{\text{total}}$ showed a tendency to improve patient selection for ePLND over prediction models using clinical risk factors. Although this result has to be validated, ^{68}Ga -PSMA-11 PET showed the potential to reduce unnecessary surgical procedures and be a valuable tool for staging intermediate to high-risk prostate cancer patients.

Acknowledgements The authors acknowledge the technicians Marlena Hofbauer and Josephine Trinckauf and their team for the excellent work on high-quality PET images.

Authors' contributions DAF—data collection, data analysis and manuscript writing.

UJM—data analysis, statistics and manuscript writing.

HIGS and TH—patient selection, manuscript writing.

NJR, EEGWV, MM, JHR and MH—manuscript editing and revision.

IAB—study design and manuscript writing.

All authors reviewed and agreed to the manuscript content.

Funding information The Department of Nuclear Medicine holds an institutional Research Contract with GE Healthcare. This study was financially supported by the Sick legat and the Iten-Kohaut foundation

Compliance with ethical standards

Ethics approval and consent to participate The local ethics committee approved the study protocol and all patients gave a general written informed consent for retrospective use of their data (BASEC Nr. 2018-01284).

Consent for publication Not applicable.

Availability of data and material Patient imaging was done in the scope of the routine clinical diagnostic studies, and the raw data are stored in the hospital archiving system at the Zurich University Hospital, Zurich, Switzerland.

Competing interests IAB has received research grants and speaker honorarium from GE Healthcare, research grants from Swiss Life and speaker honorarium from Bayer Health Care and Astellas Pharma AG. TH holds an advisory function for MSD and Bayer. MH received an Investigator-Initiated Study grant from GE Healthcare. MM received speaker fees from GE Healthcare. Authors DAF, UJM, HIGS, NJR, JHR and EEGWV declare no conflict of interest.

References

- Mottet N, Bellmunt J, Bolla M, Briers E, Cumberbatch MG, De Santis M, et al. EAU-ESTRO-SIOG guidelines on prostate cancer. Part 1: screening, diagnosis, and local treatment with curative intent. *Eur Urol*. 2017;71:618–29. <https://doi.org/10.1016/j.eururo.2016.08.003>.
- Ploussard G, Briganti A, de la Taille A, Haese A, Heidenreich A, Menon M, et al. Pelvic lymph node dissection during robot-assisted radical prostatectomy: efficacy, limitations, and complications—a systematic review of the literature. *Eur Urol*. 2014;65:7–16. <https://doi.org/10.1016/j.eururo.2013.03.057>.
- Fossati N, Willemsse PM, Van den Broeck T, van den Bergh RCN, Yuan CY, Briers E, et al. The benefits and harms of different extents of lymph node dissection during radical prostatectomy for prostate cancer: a systematic review. *Eur Urol*. 2017;72:84–109. <https://doi.org/10.1016/j.eururo.2016.12.003>.
- Bernstein AN, Shoag JE, Golan R, Halpern JA, Schaeffer EM, Hsu WC, et al. Contemporary incidence and outcomes of prostate cancer lymph node metastases. *J Urol*. 2018;199:1510–7. <https://doi.org/10.1016/j.juro.2017.12.048>.
- Briganti A, Abdollah F, Nini A, Suardi N, Gallina A, Capitanio U, et al. Performance characteristics of computed tomography in detecting lymph node metastases in contemporary patients with prostate cancer treated with extended pelvic lymph node dissection. *Eur Urol*. 2012;61:1132–8. <https://doi.org/10.1016/j.eururo.2011.11.008>.
- Hovels AM, Heesakkers RA, Adang EM, Jager GJ, Strum S, Hoogeveen YL, et al. The diagnostic accuracy of CT and MRI in the staging of pelvic lymph nodes in patients with prostate cancer: a meta-analysis. *Clin Radiol*. 2008;63:387–95. <https://doi.org/10.1016/j.crad.2007.05.022>.
- Evangelista L, Guttilla A, Zattoni F, Muzzio PC, Zattoni F. Utility of choline positron emission tomography/computed tomography for lymph node involvement identification in intermediate- to high-risk prostate cancer: a systematic literature review and meta-analysis. *Eur Urol*. 2013;63:1040–8. <https://doi.org/10.1016/j.eururo.2012.09.039>.
- von Eyben FE, Kairemo K. Meta-analysis of (11)C-choline and (18)F-choline PET/CT for management of patients with prostate cancer. *Nucl Med Commun*. 2014;35:221–30. <https://doi.org/10.1097/MNM.000000000000040>.
- Nguyen DP, Huber PM, Metzger TA, Genitsch V, Schudel HH, Thalmann GN. A specific mapping study using fluorescence sentinel lymph node detection in patients with intermediate- and high-risk prostate cancer undergoing extended pelvic lymph node dissection. *Eur Urol*. 2016;70:734–7. <https://doi.org/10.1016/j.eururo.2016.01.034>.
- Chun FK, Karakiewicz PI, Briganti A, Gallina A, Kattan MW, Montorsi F, et al. Prostate cancer nomograms: an update. *Eur Urol*. 2006;50:914–26; discussion 26. <https://doi.org/10.1016/j.eururo.2006.07.042>.
- Bianchi L, Gandaglia G, Fossati N, Suardi N, Moschini M, Cucchiaro V, et al. Pelvic lymph node dissection in prostate cancer: indications, extent and tailored approaches. *Urologia*. 2017;84:9–19. <https://doi.org/10.5301/uro.5000139>.
- Mohler JL, Armstrong AJ, Bahnsen RR, D'Amico AV, Davis BJ, Eastham JA, et al. Prostate Cancer, version 1.2016. *J Natl Compr Cancer Netw*. 2016;14:19–30.
- Briganti A, Larcher A, Abdollah F, Capitanio U, Gallina A, Suardi N, et al. Updated nomogram predicting lymph node invasion in patients with prostate cancer undergoing extended pelvic lymph node dissection: the essential importance of percentage of positive cores. *Eur Urol*. 2012;61:480–7. <https://doi.org/10.1016/j.eururo.2011.10.044>.
- Banapour P, Schumacher A, Lin JC, Finley DS. Radical prostatectomy and pelvic lymph node dissection in Kaiser Permanente Southern California: 15-year experience. *Perm J*. 2019;23. <https://doi.org/10.7812/TPP/17-233>.
- Roscigno M, Nicolai M, La Croce G, Pellucchi F, Scarcello M, Sacca A, et al. Difference in frequency and distribution of nodal metastases between intermediate and high risk prostate cancer patients: results of a superextended pelvic lymph node dissection. *Front Surg*. 2018;5:52. <https://doi.org/10.3389/fsurg.2018.00052>.
- Hope TA, Goodman JZ, Allen IE, Calais J, Fendler WP, Carroll PR. Meta-analysis of (68)Ga-PSMA-11 PET accuracy for the detection of prostate Cancer validated by histopathology. *J Nucl Med*. 2018. <https://doi.org/10.2967/jnumed.118.219501>.
- Thalgott M, Duwel C, Rauscher I, Heck MM, Haller B, Gafita A, et al. One-stop shop whole-body (68)Ga-PSMA-11 PET/MRI compared to clinical Nomograms for preoperative T- and N-Staging of High-Risk Prostate Cancer. *J Nucl Med*. 2018. <https://doi.org/10.2967/jnumed.117.207696>.
- Uprimny C, Kroiss AS, Decristoforo C, Fritz J, von Guggenberg E, Kandler D, et al. (68)Ga-PSMA-11 PET/CT in primary staging of prostate cancer: PSA and Gleason score predict the intensity of tracer accumulation in the primary tumour. *Eur J Nucl Med Mol Imaging*. 2017;44:941–9. <https://doi.org/10.1007/s00259-017-3631-6>.
- von Klot CJ, Merseburger AS, Boker A, Schmuck S, Ross TL, Bengel FM, et al. (68)Ga-PSMA PET/CT imaging predicting Intraprostatic tumor extent, extracapsular extension and seminal vesicle invasion prior to radical prostatectomy in patients with prostate cancer. *Nucl Med Mol Imaging*. 2017;51:314–22. <https://doi.org/10.1007/s13139-017-0476-7>.
- Ross JS, Sheehan CE, Fisher HA, Kaufman RP Jr, Kaur P, Gray K, et al. Correlation of primary tumor prostate-specific membrane antigen expression with disease recurrence in prostate cancer. *Clin Cancer Res*. 2003;9:6357–62.
- Bravaccini S, Puccetti M, Bocchini M, Ravaioli S, Celli M, Scarpì E, et al. PSMA expression: a potential ally for the pathologist in

- prostate cancer diagnosis. *Sci Rep.* 2018;8:4254. <https://doi.org/10.1038/s41598-018-22594-1>.
22. Uslu-Besli L, Asa S, Bakir B, Sayman H, Sager S, Khosroshahi BR, et al. Correlation of SUVmax and ADC values detected by Ga-68 PSMA PET/MRI in primary prostate lesions and their significance in lymph node metastasis. *Eur J Nucl Med Mol Imaging.* 2018;45: S20-S.
 23. Hueting TA, Cornel EB, Somford DM, Jansen H, van Basten J-PA, Pleijhuis RG, et al. External validation of models predicting the probability of lymph node involvement in prostate cancer patients. *Eur Urol Oncol.* 2018.
 24. Cagiannos I, Karakiewicz P, Eastham JA, Ohori M, Rabbani F, Gerigk C, et al. A preoperative nomogram identifying decreased risk of positive pelvic lymph nodes in patients with prostate cancer. *J Urol.* 2003;170:1798–803. <https://doi.org/10.1097/01.ju.0000091805.98960.13>.
 25. Yu JB, Makarov DV, Gross C. A new formula for prostate cancer lymph node risk. *Int J Radiat Oncol Biol Phys.* 2011;80:69–75. <https://doi.org/10.1016/j.ijrobp.2010.01.068>.
 26. Roach M 3rd, Marquez C, Yuo HS, Narayan P, Coleman L, Nseyo UO, et al. Predicting the risk of lymph node involvement using the pre-treatment prostate specific antigen and Gleason score in men with clinically localized prostate cancer. *Int J Radiat Oncol Biol Phys.* 1994;28:33–7.
 27. Winter A, Kneib T, Rohde M, Henke RP, Wawroschek F. First nomogram predicting the probability of lymph node involvement in prostate cancer patients undergoing radioisotope guided sentinel lymph node dissection. *Urol Int.* 2015;95:422–8. <https://doi.org/10.1159/000431182>.
 28. Tosoian JJ, Chappidi M, Feng Z, Humphreys EB, Han M, Pavlovich CP, et al. Prediction of pathological stage based on clinical stage, serum prostate-specific antigen, and biopsy Gleason score: Partin Tables in the contemporary era. *BJU Int.* 2017;119: 676–83. <https://doi.org/10.1111/bju.13573>.
 29. D'Amico AV, Whittington R, Malkowicz SB, Schultz D, Blank K, Broderick GA, et al. Biochemical outcome after radical prostatectomy, external beam radiation therapy, or interstitial radiation therapy for clinically localized prostate cancer. *JAMA.* 1998;280:969–74.
 30. Fendler WP, Eiber M, Beheshti M, Bomanji J, Ceci F, Cho S, et al. Ga-68-PSMA PET/CT: joint EANM and SNMMI procedure guideline for prostate cancer imaging: version 1.0. *Eur J Nucl Med Mol Imaging.* 2017;44:1014–24. <https://doi.org/10.1007/s00259-017-3670-z>.
 31. Kranzbuhler B, Nagel H, Becker AS, Muller J, Huellner M, Stolzmann P, et al. Clinical performance of (68)Ga-PSMA-11 PET/MRI for the detection of recurrent prostate cancer following radical prostatectomy. *Eur J Nucl Med Mol Imaging.* 2018;45:20–30. <https://doi.org/10.1007/s00259-017-3850-x>.
 32. Hofman MS, Hicks RJ, Maurer T, Eiber M. Prostate-specific membrane antigen PET: clinical utility in prostate cancer, normal patterns, pearls, and pitfalls. *Radiographics.* 2018;38:200–17. <https://doi.org/10.1148/rg.2018170108>.
 33. Fendler WP, Calais J, Allen-Auerbach M, Bluemel C, Eberhardt N, Emmett L, et al. (68)Ga-PSMA-11 PET/CT interobserver agreement for prostate cancer assessments: an international multicenter prospective study. *J Nucl Med.* 2017;58:1617–23. <https://doi.org/10.2967/jnumed.117.190827>.
 34. Feicke A, Baumgartner M, Talimi S, Schmid DM, Seifert HH, Muntener M, et al. Robotic-assisted laparoscopic extended pelvic lymph node dissection for prostate cancer: surgical technique and experience with the first 99 cases. *Eur Urol.* 2009;55:876–83. <https://doi.org/10.1016/j.eururo.2008.12.006>.
 35. Steyerberg EW, Vickers AJ, Cook NR, Gerds T, Gonen M, Obuchowski N, et al. Assessing the performance of prediction models: a framework for traditional and novel measures. *Epidemiology.* 2010;21:128–38. <https://doi.org/10.1097/EDE.0b013e3181c30fb2>.
 36. Vickers AJ, Elkin EB. Decision curve analysis: a novel method for evaluating prediction models. *Med Decis Mak.* 2006;26:565–74. <https://doi.org/10.1177/0272989X06295361>.
 37. Kerr KF, Brown MD, Zhu K, Janes H. Assessing the clinical impact of risk prediction models with decision curves: guidance for correct interpretation and appropriate use. *J Clin Oncol.* 2016;34:2534–40. <https://doi.org/10.1200/JCO.2015.65.5654>.
 38. Van Calster B, Wynants L, Verbeek JFM, Verbakel JY, Christodoulou E, Vickers AJ, et al. Reporting and interpreting decision curve analysis: a guide for investigators. *Eur Urol.* 2018;74: 796–804. <https://doi.org/10.1016/j.eururo.2018.08.038>.
 39. Epstein JI, Egevad L, Amin MB, Delahunt B, Srigley JR, Humphrey PA, et al. The 2014 International Society of Urological Pathology (ISUP) consensus conference on Gleason grading of prostatic carcinoma: definition of grading patterns and proposal for a new grading system. *Am J Surg Pathol.* 2016;40: 244–52. <https://doi.org/10.1097/PAS.0000000000000530>.
 40. Berglund E, Maaskola J, Schultz N, Friedrich S, Marklund M, Bergenstrahle J, et al. Spatial maps of prostate cancer transcriptomes reveal an unexplored landscape of heterogeneity. *Nat Commun.* 2018;9:2419. <https://doi.org/10.1038/s41467-018-04724-5>.
 41. Tu SM, Lin SH, Logothetis CJ. Stem-cell origin of metastasis and heterogeneity in solid tumours. *Lancet Oncol.* 2002;3:508–13.
 42. Hupe MC, Philippi C, Roth D, Kumpers C, Ribbat-Idel J, Becker F, et al. Expression of Prostate-Specific Membrane Antigen (PSMA) on biopsies is an independent risk stratifier of prostate cancer patients at time of initial diagnosis. *Front Oncol.* 2018;8:623. <https://doi.org/10.3389/fonc.2018.00623>.
 43. Blanchard P, Faivre L, Lesaunier F, Salem N, Mesgouez-Nebout N, Deniau-Alexandre E, et al. Outcome according to elective pelvic radiation therapy in patients with high-risk localized prostate cancer: a secondary analysis of the GETUG 12 phase 3 randomized trial. *Int J Radiat Oncol Biol Phys.* 2016;94:85–92. <https://doi.org/10.1016/j.ijrobp.2015.09.020>.
 44. Seaward SA, Weinberg V, Lewis P, Leigh B, Phillips TL, Roach M 3rd. Improved freedom from PSA failure with whole pelvic irradiation for high-risk prostate cancer. *Int J Radiat Oncol Biol Phys.* 1998;42:1055–62.
 45. Aizer AA, Yu JB, McKeon AM, Decker RH, Colberg JW, Peschel RE. Whole pelvic radiotherapy versus prostate only radiotherapy in the management of locally advanced or aggressive prostate adenocarcinoma. *Int J Radiat Oncol Biol Phys.* 2009;75:1344–9. <https://doi.org/10.1016/j.ijrobp.2008.12.082>.
 46. Roach M, Moughan J, Lawton CAF, Dicker AP, Zeitzer KL, Gore EM, et al. Sequence of hormonal therapy and radiotherapy field size in unfavourable, localised prostate cancer (NRG/RTOG 9413): long-term results of a randomised, phase 3 trial. *Lancet Oncol.* 2018;19: 1504–15. [https://doi.org/10.1016/S1470-2045\(18\)30528-X](https://doi.org/10.1016/S1470-2045(18)30528-X).
 47. Daoud MA, Aboelnaga EM, Alashry MS, Fathy S, Aletreby MA. Clinical outcome and toxicity evaluation of simultaneous integrated boost pelvic IMRT/VMAT at different dose levels combined with androgen deprivation therapy in prostate cancer patients. *Oncol Targets Ther.* 2017;10:4981–8. <https://doi.org/10.2147/OTT.S141224>.
 48. Ishii K, Ogino R, Hosokawa Y, Fujioka C, Okada W, Nakahara R, et al. Comparison of dosimetric parameters and acute toxicity after whole-pelvic vs prostate-only volumetric-modulated arc therapy

- with daily image guidance for prostate cancer. *Br J Radiol.* 2016;89:20150930. <https://doi.org/10.1259/bjr.20150930>.
49. White KL, Varrassi E, Routledge JA, Barraclough LH, Livsey JE, McLaughlin J, et al. Does the use of volumetric modulated arc therapy reduce gastrointestinal symptoms after pelvic radiotherapy? *Clin Oncol (R Coll Radiol).* 2018;30:e22–e8. <https://doi.org/10.1016/j.clon.2017.10.016>.
50. Choo MS, Kim M, Ku JH, Kwak C, Kim HH, Jeong CW. Extended versus standard pelvic lymph node dissection in radical prostatectomy on oncological and functional outcomes: a systematic review and meta-analysis. *Ann Surg Oncol.* 2017;24:2047–54. <https://doi.org/10.1245/s10434-017-5822-6>.

Publisher's note Springer Nature remains neutral with regard to jurisdictional claims in published maps and institutional affiliations.